J. Mech. Phys. Solids Vol. 37, No. 4, pp. 515–540, 1989.
Printed in Great Britain.

0022–5096/89 $3.00 + 0.00

SOFTENING BY VOID NUCLEATION AND GROWTH IN TENSION AND SHEAR

N. A. FLECK

Department of Engineering, University of Cambridge, Cambridge CB2 1PZ, U.K.

J. W. HUTCHINSON

Division of Applied Sciences, Harvard University, Cambridge, MA 02138, U.S.A.

and

V. TVERGAARD

Department of Solid Mechanics, The Technical University of Denmark, DK-2800 Lyngby, Denmark

(*Received* 8 *June* 1988)

ABSTRACT

THE EFFECT of void nucleation and growth on overall stress–strain behavior is investigated for solids undergoing plastic straining under axisymmetric and shearing conditions. Contact between the void surface and the nucleating particle is taken into account and is found to be important under shear and under axisymmetric straining when the stress triaxiality is low. The notion of the macroscopic stress drop due to nucleation of a void is defined and computed, both for isolated voids and for voids in periodic arrays. The stress drop for an isolated void in an infinite matrix can be used to predict softening due to void nucleation when the void concentration is dilute. Interaction between voids in shear during nucleation is analysed numerically and softening effects are calculated along with large strain aspects of void deformation during subsequent growth.

1. INTRODUCTION

THE EFFECT of nucleation and growth of voids on the overall tensile stress–strain behavior of an elastic–plastic solid is depicted in Fig. 1. If voids nucleate by debonding or cracking of particles starting at a strain E_N, the overall stress–strain behavior then begins to display softening relative to a comparison material whose particles do not debond or crack. Each particle sheds part or all of its load when it nucleates a void and this results in a drop in the overall stress at a given overall strain. Once a void is nucleated its further growth makes an additional contribution to softening. Softening due to void growth is proportional to the void volume fraction ρ and therefore only becomes significant somewhat after the onset of nucleation.

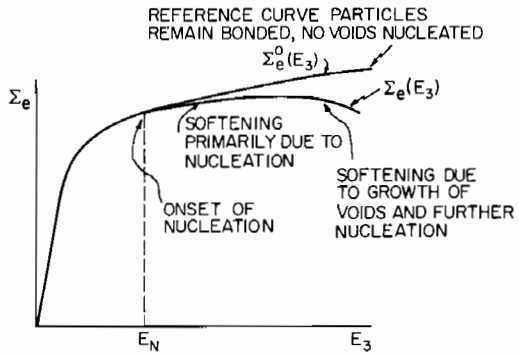

FIG. 1. Effect of void nucleation and subsequent growth on macroscopic tensile stress–strain behavior.

To fix these notions more firmly and to set the background for the work contained within, let $\Sigma_e^0(E_3)$ denote the overall effective stress at strain E_3 under axisymmetric straining for a matrix material containing rigid spherical particles which do not debond. In the next section, we define and compute the deviator stress drop $\Delta\boldsymbol{\Sigma}'$ associated with the nucleation of a void by debonding of an isolated spherical particle of unit volume in an infinite elastic–perfectly plastic matrix. The result has the form

$$\Delta\Sigma'_{ij} = \tfrac{2}{3}F(X)\Sigma'_{ij}, \tag{1.1}$$

where $\boldsymbol{\Sigma}$ is the remote stress and $\boldsymbol{\Sigma}'$ is its deviator. The stress drop is a strong function of the stress triaxiality $X = \Sigma_m/\Sigma_e$ where

$$\Sigma_m = \tfrac{1}{3}\Sigma_{kk} \quad \text{and} \quad \Sigma_e = (3\Sigma'_{ij}\Sigma'_{ij}/2)^{1/2}. \tag{1.2}$$

Suppose under proportional axisymmetric stressing that at strain E_3 voids have been nucleated at some of the particles corresponding to a void volume fraction ρ. If the distribution of the voids can be regarded as dilute, the overall effective stress can be estimated using the stress drop (1.1) as

$$\Sigma_e(E_3) = [1 - \tfrac{2}{3}\rho F(X)]\Sigma_e^0(E_3). \tag{1.3}$$

The tangent modulus of the overall effective stress–strain at fixed triaxiality is

$$E_t = \frac{\mathrm{d}\Sigma_e}{\mathrm{d}E_3} = E_t^0[1 - \tfrac{2}{3}\rho F] - \tfrac{2}{3}F\Sigma_e^0\frac{\mathrm{d}\rho}{\mathrm{d}E_3}, \tag{1.4}$$

where $E_t^0 = \mathrm{d}\Sigma_e^0/\mathrm{d}E_3$ is the tangent modulus of the material with all particles bonded at E_3. During any increment of strain, $\dot{E}_3$, ρ increases due to nucleation of new voids, $\dot{\rho}_N$, and growth of previously nucleated voids, $\dot{\rho}_G$, so that

$$\frac{\mathrm{d}\rho}{\mathrm{d}E_3} = \frac{\mathrm{d}\rho_N}{\mathrm{d}E_3} + \frac{\mathrm{d}\rho_G}{\mathrm{d}E_3}, \tag{1.5}$$

where results such as those of RICE and TRACEY (1969) give the triaxiality dependence of void growth in the form

$$\frac{d\rho_G}{dE_3} = \rho f(X) \tag{1.6}$$

for dilute distribution of voids. Thus the erosion of the incremental stiffness of the material has a contribution

$$-\tfrac{2}{3}F\Sigma_e^0(d\rho_N/dE_3) \tag{1.7}$$

due to nucleation and a contribution

$$-\tfrac{2}{3}\rho F f \Sigma_e^0 \tag{1.8}$$

due to growth of existing voids. At the onset of nucleation the reduction in stiffness is due entirely to nucleation since $\rho = 0$.

The above features have all been included in the Gurson model of dilatant plasticity (GURSON, 1977; NEEDLEMAN and RICE, 1978). One of the objectives of the present paper is to provide results which permit an assessment of phenomenological theories such as the Gurson model. The present study is carried out within the framework of continuum plasticity theory on the assumption that the particles and the voids nucleated from them are large in size compared to dislocation cell size. The continuum theory of plasticity cannot be used to predict hardening due to precipitates whose size and spacing is comparable to the distance between dislocations. Similarly it cannot predict softening due to nucleation or growth of voids which are too small.

In Section 2 the basic problem is considered for nucleation and initial growth of a void from an isolated rigid spherical particle. The functions $F(X)$ and $f(X)$ in (1.1) and (1.6) are calculated for axisymmetric remote stress states. Results for these functions which account for contact between void surface and particle are contrasted with those which ignore particle contact. Interaction between the void surface and its nucleating particle are expected to be particularly important under shear since an unrestrained void closes up as it deforms in a shear field. Softening due to void nucleation and growth in shear are analysed in Sections 3 and 4. A two-dimensional plane strain model of a periodic array of interacting void-nucleating particles in an elastic–perfectly plastic matrix is analysed in Section 3. The evolution of three-dimensional voids in a linear viscous material in simple shear is considered in Section 4. The emphasis throughout the paper is on the effect of nucleation and subsequent growth on overall stress–strain behavior.

2. Nucleation and Initial Growth of a Void From an Isolated Rigid Spherical Particle

2.1. *Formulation of problem*

The matrix material is assumed to be elastic–perfectly plastic with tensile yield stress σ_0 and a Mises yield condition $\sigma_e = \sigma_0$ where $\sigma_e = (3\sigma'_{ij}\sigma'_{ij}/2)^{1/2}$ is the effective stress and σ'_{ij} is the stress deviator. The material is taken to be elastically isotropic with Young's modulus E, and for computational convenience it is assumed to be elastically incompressible. For plastic loading ($\sigma_e = \sigma_0$ and $\dot{\sigma}_e = 0$) the plastic strain rate is

$$\varepsilon^p_{ij} = \dot{\beta}\sigma'_{ij}, \quad \dot{\beta} \geqslant 0 \tag{2.1}$$

and otherwise vanishes. Prior to nucleation, the rigid spherical particle is bonded to an infinite matrix of this material. The remote stress and strain rate are denoted by $\boldsymbol{\Sigma}$ and $\dot{\mathbf{E}}$ and these are taken to be axisymmetric (see Fig. 2) such that

$$\Sigma_{33} = S, \quad \Sigma_{11} = \Sigma_{22} = T \quad \text{with} \quad S > T. \tag{2.2}$$

For remote yielding, $S-T = \sigma_0$ and

$$\dot{E}_{33} = -\tfrac{1}{2}\dot{E}_{11} = -\tfrac{1}{2}\dot{E}_{22} > 0. \tag{2.3}$$

The measure of remote triaxiality defined in the introduction is

$$X = \Sigma_m/\Sigma_e = (S+2T)/(3\sigma_0). \tag{2.4}$$

Suppose the remote stresses are applied proportionally until remote yield occurs with further straining until the limit stress distribution in the matrix $\boldsymbol{\sigma}^0(\mathbf{x})$ is attained. The traction across the particle–matrix interface is $T_{ij}^0 = \sigma_{ij}^0 n_j$. If the triaxiality is sufficient to ensure that the void surface pulls away from the particle at every point, nucleation is modeled by incrementally reducing the traction on the particle to zero. During this nucleation process the remote strain is increased by an amount δE_N. That is, if the radial velocity of the matrix interface is such that the void pulls away completely from the particle, nucleation is modeled by a sequence of quasi-static incremental problems whose boundary conditions are

$$\dot{\sigma}_{ij} n_j = -\dot{\lambda}\sigma_{ij}^0 n_j \quad \text{on} \quad A_0 \quad \text{and} \quad \dot{E}_3 = \dot{\lambda}\delta E_N, \tag{2.5}$$

where $\lambda = 0$ at the start of nucleation and $\lambda = 1$ at the finish. The intent of the analysis of nucleation in this paper is not to represent realistically the debonding process which is thought to involve interfacial separation by dynamic crack growth in many cases. Instead, our aim is to predict the consequences of nucleation at the macroscopic level. An earlier paper (HUTCHINSON and TVERGAARD, 1987) established that the overall stress and strain behavior was rather insensitive to the details of the nucleation process itself, as will be discussed further below. NEEDLEMAN (1987) has formulated a model of particle debonding which more faithfully deals with interfacial separation between particle and matrix.

Below a certain level of remote triaxiality (typically about $X = 0.6$ but depending

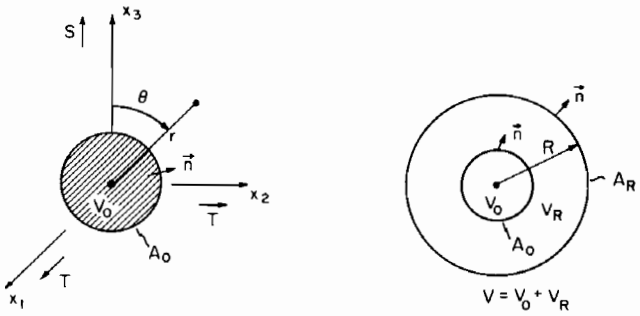

FIG. 2. Geometry and conventions for isolated void calculations.

somewhat on δE_N) the radial velocity of the void surface is found to be negative in the vicinity of the equator of the particle ($\theta = \pi/2$) when the unconstrained boundary conditions (2.5) are applied. Contact between void surface and particle is approximated in the following way. During any incremental step with conditions (2.5) in effect in which it is found that the radial velocity at the equator is negative, the boundary conditions (2.5) are supplemented by a constraint on the velocity fields which ensures that the radial velocity at the equator is zero. The full analysis, which is similar in some of its details to the earlier analysis of HUTCHINSON and TVERGAARD (1987), is outlined in the Appendix.

2.2. *The stress drop*

The quantities of primary interest which will be reported below are the volume change of the void and the stress drop. The stress drop is now defined along with the equation used for computing it. Consider for a moment a rigid particle of unit volume in a matrix with finite outer radius R, as illustrated in Fig. 2. The outer surface A_R is subject to uniform straining with $\dot{u}_i = \dot{E}_{ij}x_j$ where $\dot{E}_{kk} = 0$. Otherwise, the nucleation problem and subsequent initial growth problem are as described above. Let the stress distribution at any stage of the process be $\boldsymbol{\sigma}(\mathbf{x})$ and define the overall, or average, stress of the composite body in the usual way as

$$V\Sigma_{ij} = \int_{A_R} \sigma_{ik} n_k x_j \, \mathrm{d}A. \tag{2.6}$$

Let $\boldsymbol{\sigma}^0(\mathbf{x})$ be the limit stress distribution for the same configuration where the rigid particle is bonded to the matrix and where the same uniform straining, $\dot{u}_i = \dot{E}_{ij}x_j$, is applied to A_R. At any stage in the nucleation process or thereafter during the growth phase, the *stress drop* relative to the overall stress for the bonded particle is defined as

$$\Delta\Sigma_{ij} = \int_{A_R} (\sigma^0_{ik} - \sigma_{ik}) n_k x_j \, \mathrm{d}A, \tag{2.7}$$

where it is understood that the particle has a unit volume.

To compute the deviator stress drop under axisymmetric conditions it is convenient to work with a scalar equation which derives from (2.7). With $\dot{\mathbf{u}}$ as the velocity field with strain rates $\dot{\boldsymbol{\varepsilon}}$ (with $\dot{u}_i n_i = 0$ on portions of A_0 where contact occurs), it readily follows from the principle of virtual work that

$$\begin{aligned} \Delta\Sigma_{ij}\dot{E}_{ij} &= \int_{A_R} (\sigma^0_{ik} - \sigma_{ik}) n_k \dot{u}_i \, \mathrm{d}A \\ &= \int_{V_R} (\sigma^0_{ij} - \sigma_{ij}) \dot{\varepsilon}_{ij} \, \mathrm{d}V + \int_{A_0} (\sigma^0_{ij} - \sigma_{ij}) n_j \dot{u}_i \, \mathrm{d}A \end{aligned} \tag{2.8}$$

where the conventions are noted in Fig. 2. The advantage of (2.8) is that the problem for the infinite matrix ($R \to \infty$) can be used to compute $\Delta\Sigma_{ij}\dot{E}_{ij}$ because $(\sigma^0_{ij} - \sigma_{ij})\dot{\varepsilon}_{ij}$

decays like r^{-6} for large r. Since $E_{kk} = 0$, (2.8) gives no information on $\Delta\Sigma_{kk}$. For the axisymmetric problem of Fig. 2 there is only one independent component of the deviator stress drop and it is given by

$$\Delta\Sigma'_{33} = \tfrac{2}{3}(\Delta\Sigma_{ij}\dot{E}_{ij})/\dot{E}_{33}. \tag{2.9}$$

Subsequent to nucleation during the initial growth phase the condition (2.5) on A_0 is replaced by $\dot{\sigma}_{ij}n_j = 0$ assuming no contact occurs. If contact at the equator is indicated by the unconstrained solution the radial velocity at the equator is constrained to be zero. The calculations described above can legitimately be carried out using a small strain theory of plasticity since the changes in strain and in void shape and size during nucleation are small. The same is true for the initial growth stages immediately after nucleation.

For completeness we also report the deviator *stress rise* for bonded rigid particles of unit volume relative to the pure matrix material subject to the same remote straining $\dot{\mathbf{E}}$ and with uniform stress $\boldsymbol{\Sigma}$. The deviator stress rise relative to the uniform matrix can similarly be computed from

$$\Delta\Sigma^0_{ij}\dot{E}_{ij} = \int_{V_R} (\sigma^0_{ij} - \Sigma_{ij})\dot{\varepsilon}_{ij}\,\mathrm{d}V, \tag{2.10}$$

where $\dot{\mathbf{u}} = 0$ on A_0 and where the limit problem ($R \to \infty$) can be used in the evaluation of the integral. The deviator stress rise for the bonded rigid particle is independent of remote triaxiality since the matrix is incompressible. For axisymmetric straining the computed value is (see Appendix for details)

$$\Delta\Sigma'_{33} = 0.32\sigma_0. \tag{2.11}$$

For a dilute distribution of bonded, rigid spherical particles with volume fraction ρ this result implies that the overall flow stress for axisymmetric straining is increased above σ_0 by $\frac{3}{2}\rho\Delta\Sigma'_{33}$, i.e.

$$\Sigma^0_e = \sigma_0[1 + 0.48\rho]. \tag{2.12}$$

This is precisely the dilute prediction obtained by DUVA (1984) who considered strengthening of power law solids by rigid spheres and who obtained (2.12) by extrapolating to the perfectly plastic limit.

Particles large enough such that their interaction with the matrix can be characterized by continuum plasticity are thus rather ineffective strengthening agents. By contrast, the softening associated with voids nucleated from such particles is appreciably larger, as will be seen.

2.3. *Numerical results for nucleation*

Two nucleation and initial growth histories are displayed in Fig. 3 for the case where $\delta E_N = 2\varepsilon_0$ with $\varepsilon_0 = \sigma_0/E$. The computational procedure for these results and others in this section are discussed in the Appendix. During the history for which the remote stress triaxiality is $X = 1$ the void pulls away from the particle immediately at the start of nucleation and never again contacts the particle. For $X = 1/3$ (remote

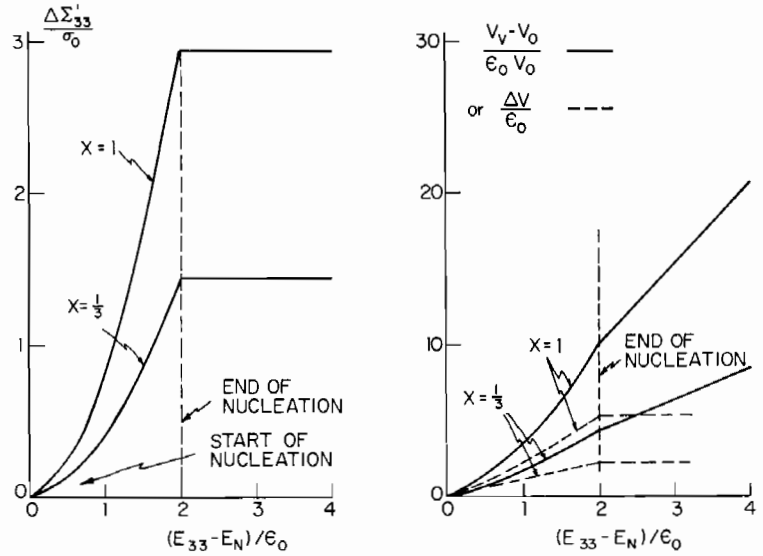

FIG. 3. Stress drop history and volume increase for nucleation and initial growth of a void from a rigid spherical particle of unit volume ($X = 1/3$ and 1, $\delta E_N = 2\varepsilon_0$).

uniaxial tension) the void surface remains in contact with the equator of the particle during nucleation and subsequent growth. In both instances, the stress drop at the end of nucleation is virtually the same, to within 1%, as the stress drop attained after additional straining. Moreover, the stress drop at the end of nucleation is essentially independent of δE_N for all δE_N greater than about $2\varepsilon_0$, as documented by HUTCHINSON and TVERGAARD (1987). For δE_N less than $2\varepsilon_0$ the stress drop is larger than that shown but rapidly attains the values shown after small further straining on the order of ε_0.

The normalized volume increase of the void $(V_v - V_0)/(\varepsilon_0 V_0)$, is shown in Fig. 3, where V_v and V_0 are the current and initial volumes. Also shown is that part of the normalized volume change which is due just to nucleation, i.e. that part which is due to relaxation of the tractions on the particle–void interface in (2.5) independent of the contribution due to the increase in E_3 during nucleation. The two parts are easily separated in the calculation of $\dot{V}_v$ and the part due to nucleation is again essentially independent of δE_N. The volume change due to nucleation is denoted by ΔV and is defined for nucleation from a particle of unit volume.

For axisymmetric stress states with $S > T$ the deviator stress drop relative to the bonded particle of unit volume can be written as

$$\Delta\Sigma'_{ij} = \tfrac{2}{3}F(X)\Sigma'_{ij}, \tag{2.13}$$

in accord with the notation introduced by HUTCHINSON and TVERGAARD (1987), where $\Sigma'_{33} = 2\sigma_0/3$. Selected values of $F(X)$ calculated with $\delta E_N = 2\varepsilon_0$ are given in Table 1 and $F(X)$ is plotted in Fig. 4. The velocity constraint at the equator of the particle operates during nucleation for stress triaxiality less than about $X = 0.6$. However, the effect of the constraint is quite small for $X > 1/3$, as was ascertained by repeating the calculation with no constraint (see values reported in Table 1). Included

TABLE 1. $F(X)$

X	$F^{(1)}$	$F^{(2)}$	$F^{(3)}$
−0.5	1.73	3.36	3.01
−0.3	1.88	3.04	2.31
−0.1	2.17	2.92	2.20
0.048	2.48	2.96	2.24
0.167	2.77	3.08	2.35
0.333	3.26	3.37	2.64
0.583	4.13	4.15	3.41
1.0	6.63	6.63	5.90
1.333	10.3	10.3	9.59
1.833	20.5	20.5	19.8

$F^{(1)}$—nucleation from rigid particle accounting for contact.
$F^{(2)}$—nucleation from rigid particle not accounting for contact.
$F^{(3)}$—nucleation from uniform stress state not accounting for contact.

in Fig. 4 is the result of a calculation, as carried out earlier by HUTCHINSON and TVERGAARD (1987), which nucleates the void from a uniform stress state (i.e. $\boldsymbol{\sigma}^0 = \boldsymbol{\Sigma}$ in the above) rather than from the non-uniform stress distribution induced by the rigid particle. The earlier calculation also ignores contact between void surface and particle. For stress triaxiality greater than uniaxial tension ($X > 1/3$) the difference between the curve of the earlier analysis and the present one is almost entirely accounted for by the stress rise (2.11) associated with the rigid particle relative to the uniform matrix. The stress rise makes a contribution of $F = 0.73$, independent of X.

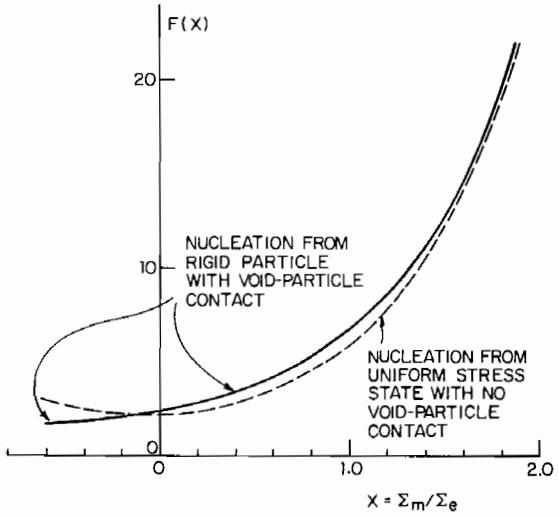

FIG. 4. Triaxiality dependence of the deviatoric stress drop in (2.13).

Even at low triaxiality, the stress drop due to nucleation of a void is about three times as large as the stress rise (2.11) due to the bonded particle. At higher triaxiality the stress rise is very small compared to the stress drop. Below $X = 1/3$ the effect of contact between the particle and void surface becomes increasingly important. For example at $X = -1/2(T = -5S)$, $F = 1.73$ when contact is accounted for and $F = 3.36$ when it is not.

The volume increase due to nucleation ΔV for a particle of unit volume can be written as

$$\Delta V = g(X)\varepsilon_0 \tag{2.14}$$

for axisymmetric loading with $S > T$. Plots of $g(X)$ are given in Fig. 5 along with the earlier predictions for nucleation from a uniform state. The volume increase due to nucleation is controlled by the elasticity of the material. A purely elastic nucleation with no contact corresponds to $\Delta V = (9/4)X\varepsilon_0$. Thus, the volume increase due to nucleation at $X = 1$ is only about twice the purely elastic value. The volume change due to nucleation is therefore generally negligible compared to the volume of the voids nucleated, i.e. $\rho\Delta V$ compared to ρ.

The earlier study of HUTCHINSON and TVERGAARD (1987) emphasized the role of the extra strain $\Delta\mathbf{E}$ produced by nucleation at a prescribed overall stress level. For nucleation in an isotropic hardening material (J_2 flow theory) the extra strain is related to the stress drop by

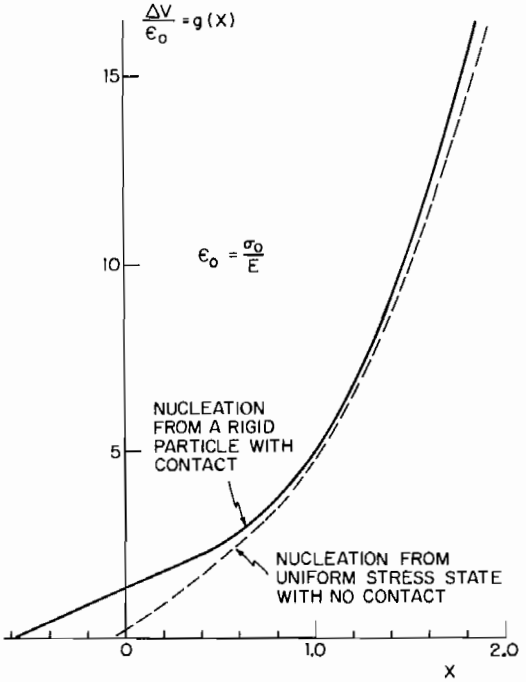

FIG. 5. Volume increase due to nucleation of a void from a particle of unit volume.

$$\Delta E_{ij} = M_{ijkl}\Delta\Sigma'_{kl} + \tfrac{1}{3}\Delta V\delta_{ij}, \tag{2.15}$$

where M is the tensor of instantaneous compliances of the matrix remote from the void. The earlier study revealed that the stress drop was essentially independent of hardening rate over a wide range of tangent moduli. Thus in this paper we have placed emphasis on the stress drop and have exploited perfect plasticity to calculate it.

An important aspect of hardening which did emerge in the earlier work was the strong dependence of the stress drop on whether isotropic hardening or kinematic hardening was assumed. For kinematic hardening based on a translating Mises yield surface with σ_0 as the *initial yield stress*, (2.13) is replaced by

$$\Delta\Sigma'_{ij} = \tfrac{2}{3}F(X, Y)\Sigma'_{ij}, \tag{2.16}$$

where $Y = \Sigma_e/\sigma_0$. Curves of F vs X are shown in Fig. 6 for three levels of Y for nucleation from a uniform state taken from the earlier study. It remains to be seen whether the strong dependence of the stress drop on hardening indicated by the kinematic hardening theory is borne out by experiments.

2.4. *Numerical results for initial growth*

Numerical results such as those in Fig. 3 indicate that there is a unique stress drop associated with an isolated spherical void of given volume which is attained at the end of the nucleation stage. It is this observation which justifies an equation like (1.3) for the overall effective stress in terms of the (dilute) void volume fraction. In a similar

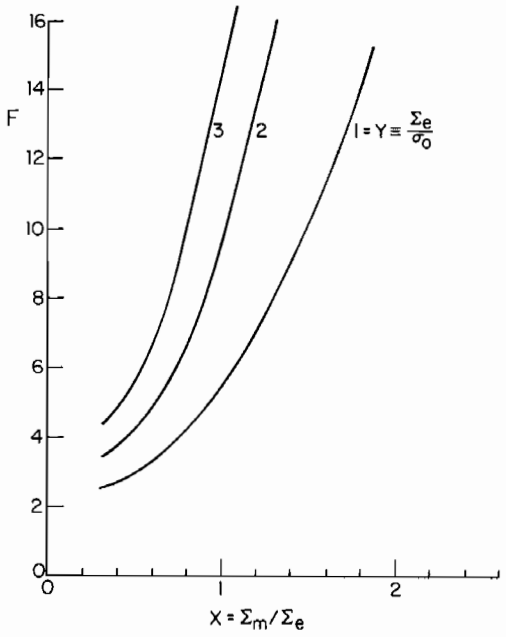

FIG. 6. Triaxiality dependence of the deviatoric stress drop in (2.16) determined using kinematic hardening theory from HUTCHINSON and TVERGAARD (1987).

fashion, the dilatation rate of the void remains constant once it is nucleated, at least until significant shape changes develop. The normalized dilatation rate of the void following nucleation

$$\frac{\dot{V}_v}{V_v \dot{E}_3} = f(X) \tag{2.17}$$

is shown in Fig. 7. The curve for the unconstrained void which neglects contact between the void surface and particle is the numerical result of RICE and TRACEY (1969). For values of X less than about 0.6 the particle props open the void and increases its dilatation rate. In uniaxial tension ($X = 1/3$) the effect of the particle increases the dilatation rate by about 45% above that for the freely deforming void. At low triaxialities, involving pressure superimposed on uniaxial tension, as in the experimental investigations of void nucleation and growth of BROWNRIGG *et al.* (1983), both the stress drop due to nucleation and the dilatation rate during subsequent growth are strongly influenced by the interaction between the particle and the void surface.

3. NUCLEATION OF VOIDS FROM CYLINDRICAL PARTICLES IN SIMPLE SHEAR

The issues addressed in the previous section are now reconsidered for the case of shear driven nucleation and growth of voids. Contact between particle and void surface are expected to be important in simple shear because an unfettered void closes

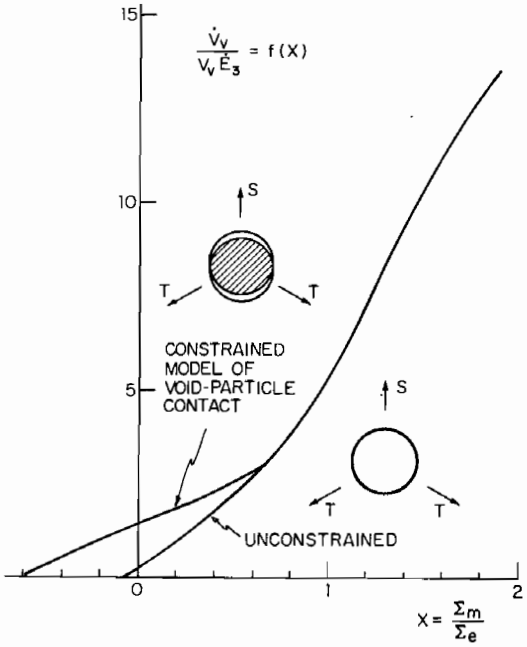

FIG. 7. Normalized dilatation rate following nucleation as a function of stress triaxiality.

as it deforms. An analysis along the lines of the previous section for nucleation of a spherical particle has not been attempted for simple shear since the problem is inherently three-dimensional and far more computationally intensive than the axisymmetric problem. In this section the two-dimensional analog problem will be analysed corresponding to nucleation of a void from a rigid, circular cylindrical particle.

The plane strain geometry analysed is shown in Fig. 8. This geometry is chosen to model experiments of COWIE, AZRIN and OLSON (1987) in which the type of test specimen sketched in Fig. 8c is subjected to shear loading along the x_1-direction combined with tension or compression in the x_2-direction. Final failure in these specimens occurs by shear localization and void sheet fracture along a plane parallel to the x_1-axis. This is modeled in the analysis by considering a row of cylindrical inclusions, which interact with one another. Since the solution is periodic, the cells indicated in Fig. 8 undergo identical behavior. The plane strain assumption of zero straining in the x_3-direction is not quite realistic for the test specimen, but is used here for convenience. The specimen shape prevents overall straining in the x_1-direction, and this is prescribed as a boundary condition.

The calculations are carried out for an elastic–perfectly plastic solid within the finite strain framework using a finite element formulation. The overall stress and void growth following nucleation are computed with an eye to discovering whether "softening" due to void deformation, as opposed to nucleation, occurs in simple shear. We return to this issue in Section 4 where three-dimensional voids subject to shear are analysed for isolated voids in linearly viscous materials.

The circular cylindrical particles in Fig. 8 are rigid with radius a and arranged with initial spacing $2b$ from center to center in the x_1-direction. The initial separation of the lower edge from the upper edge is $2c$. The layer is loaded by prescribing a uniform displacement $u_1 = \delta$ of the top edge relative to the bottom edge, together with a uniform normal true stress Σ_{22} on the two edges. The true shear stress Σ_{12} is calculated as the average of the traction in the 1-direction on the top edge, and the average straining in the x_1-direction is specified to be zero. The measure of overall shear strain was taken to be

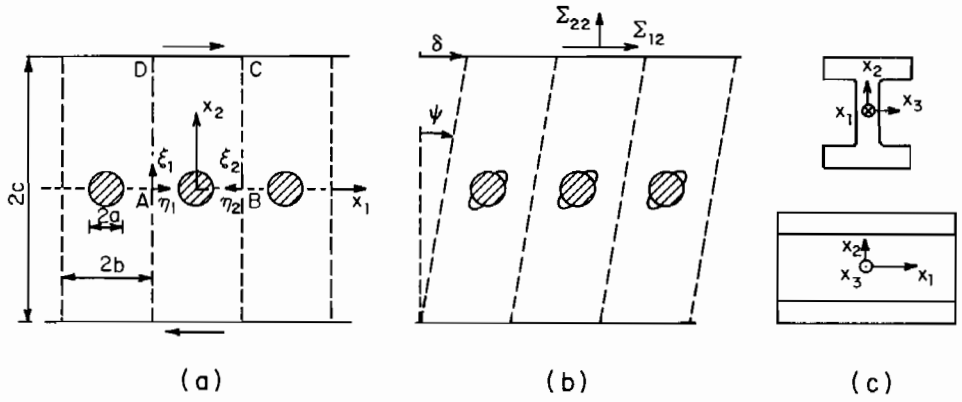

FIG. 8. Model for nucleation and a growth of 2-D voids in simple shear. (a) Starting geometry. (b) Subsequent to nucleation. (c) Test specimen modeled.

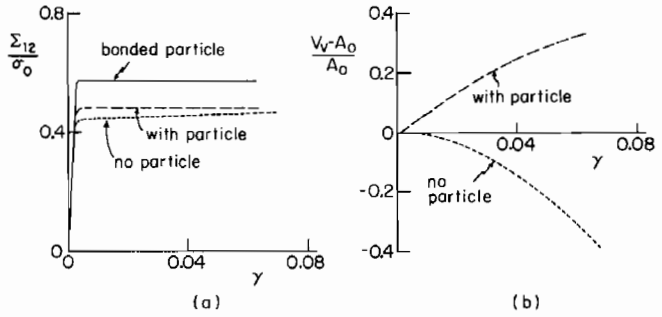

FIG. 9. Effect of early void nucleation, at $\gamma = 0$, for $a/b = 0.25$ and $\Sigma_{22} = 0$.

$$\gamma = \tan\psi = \delta/2c. \tag{3.1}$$

As in the previous section, tensile yield stress is denoted by σ_0, the yield surface is specified by the Mises invariant, and E is Young's modulus. In this section the material is elastically compressible with Poisson's ratio ν.

In the numerical solution for the periodic array of voids considered here it is only necessary to analyse the region ABCD shown in Fig. 8a. The finite strain formulation applied for the perfectly plastic material and the manner in which the periodicity conditions are incorporated in the numerical solution are described in detail in the Appendix. The particles are represented as rigid, circular cylindrical bodies, and the particle rotation due to shearing of the surrounding material is accounted for in the numerical solution. At nucleation all points of the void surface are assumed to debond simultaneously, and any subsequent contact between the particle and the void surface is represented as frictionless sliding (see Appendix). Cases are also analysed in which the voids are present from the start with no particle.

Various overall shear stress–strain curves are presented in Figs 9 and 10. In these two figures $\Sigma_{22} = 0$, $c/b = 3$, $a/b = 0.25$, $\sigma_0/E = 0.002$ and $\nu = 0.3$. Figure 9 displays a comparison of the overall curve when the particle remains bonded throughout the deformation with overall behavior when the void is nucleated at zero strain. Also included in Fig. 9 is the overall behavior for a traction-free void present from the start of straining which is free to deform with no constraint. The cross-sectional area change

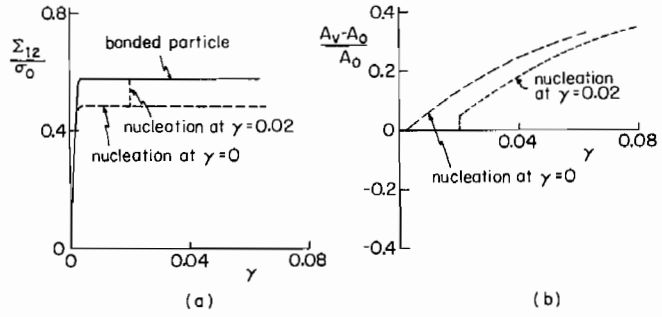

FIG. 10. Early void nucleation, at $\gamma = 0$, compared with nucleation in the fully plastic range, at $\gamma = 0.02$, for $a/b = 0.25$ and $\Sigma_{22} = 0$. Both cases account for a particle inside the void.

of the void $(A_v - A_0)$ normalized by the initial area A_0 is shown on the right in Fig. 9. The overall shear stress for the case in which the void contacts the particle is virtually independent of γ even up to volume changes of more than 30% and extensive deformation of the void. The initial shear stress drop (relative to the overall shear stress when the particles are bonded) for the case in which there is no particle inside the void is larger than that where the particle contacts the void. The ratio of these two shear stress drops is very close to the corresponding ratio for the axisymmetric case in Fig. 4 when $\Sigma_m = 0$. The overall shear stress when the voids deform freely shows a gradual, but small, increase with increasing strain γ. Strain softening due to void interaction, which might be expected, does not occur. Even in the case with a particle, where the void grows due to the contact condition, no reduction of the shear stress occurs in the range of γ-values considered. This issue will be raised again in the next section.

Figure 11 shows the initial mesh used for the numerical analysis, and two deformed meshes corresponding to the analysis for $\Sigma_{22} = 0$ illustrated in Fig. 9. For the case with no particle, Fig. 11b shows the deformations at $\gamma = 0.052$, while Fig. 11c shows the deformations at $\gamma = 0.047$ in the case where the void surface is in sliding contact with the particle. Figure 11b and c clearly show that the void volume decays in the absence of a particle, while a particle inside the void enforces a volume increase, as also shown in Fig. 9b. Both deformed meshes show that the shear deformations are highly localized in the plane containing the centers of the voids, and thus the local shear strain is much higher than the overall shear strain γ defined by (3.1). In fact, most of the shear deformations are localized in a single row of elements and it must be expected that this band of intense shear deformations would be more narrow if a finer mesh had been used.

The effect of nucleating the voids in the fully plastic state at $\gamma = 0.02$ in the presence of the particle is shown in Fig. 10. The overall stress following nucleation has been reduced to essentially the same level as for the case when the void is nucleated at $\gamma = 0$.

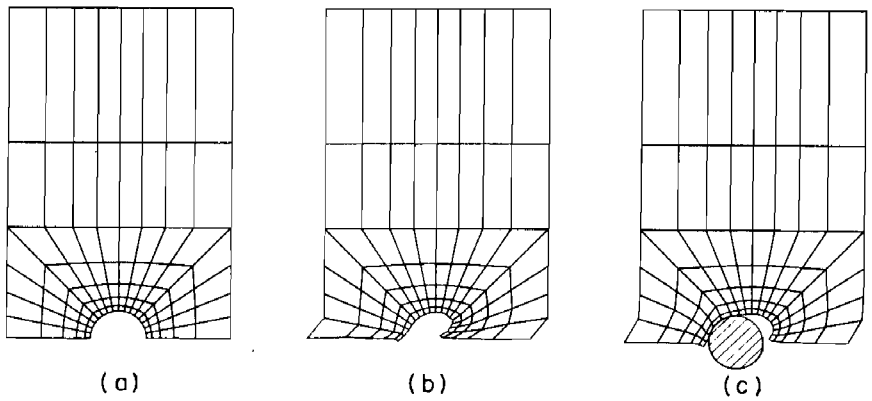

FIG. 11. (a) Initial mesh used for $a/b = 0.25$ and $c/b = 3$. (b) Deformed mesh at $\gamma = 0.052$, for $\Sigma_{22} = 0$ and no particle. (c) Deformed mesh at $\gamma = 0.047$, for $\Sigma_{22} = 0$ with a particle inside the void.

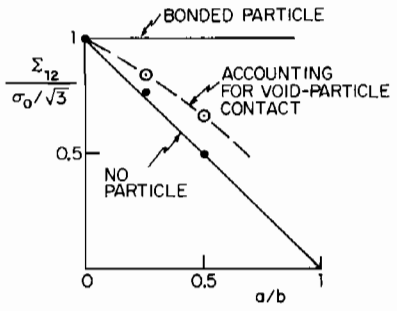

FIG. 12. Variation of the flow stress Σ_{12} with a/b for nucleated voids with and without particles present for $\Sigma_{22} = 0$. Also shown is the effect of the bonded particles on Σ_{12}.

A plot of the overall shear stress following nucleation as a function of a/b is given in Fig. 12, both for the case where contact between the void surface and particle is taken into account and for the case where the particle is "dissolved" at nucleation. With no particle present the assumption of a slip band on the plane connecting the void centers gives an upper bound to the limit load, which varies linearly with a/b, vanishing as $a/b \to 1$. Figure 12 shows that the stresses found numerically are slightly above the line, which is expected since the mesh cannot accurately resolve the slip band field leading to the upper bound estimate. The shear stresses are higher when there is a particle inside the nucleated void, but clearly the values are identical at the ends, $a/b = 0$ and $a/b = 1$.

The effect of the normal component of stress, Σ_{22}, on the overall shear stress and the void growth is shown in Fig. 13. Here, the stress Σ_{22} is applied first and then held constant as the material is subjected to shear loading. With no particle the stress drop due to the void is about the same for positive and negative values of Σ_{22}. However, for compressive Σ_{22} the void closes with increasing γ and the tendency for Σ_{12} to increase with γ is accentuated. For tensile Σ_{22} the void opens and Σ_{12} decays slightly. Interaction with the particle is exceptionally strong when $\Sigma_{22} = -\sigma_0/2$. There is very little stress drop due to nucleation since the void remains in contact with the particle over much of its surface. By contrast, the void pulls away from the particle over most of its surface when $\Sigma_{22} = \sigma_0/2$ and the behavior is much like that for unconstrained

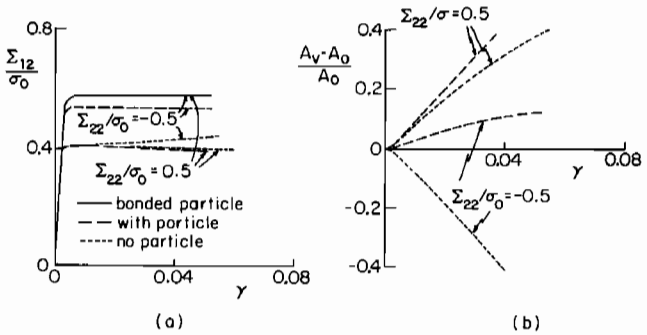

FIG. 13. Effect of a superposed normal stress Σ_{22} for $a/b = 0.25$, with nucleation at $\gamma = 0$.

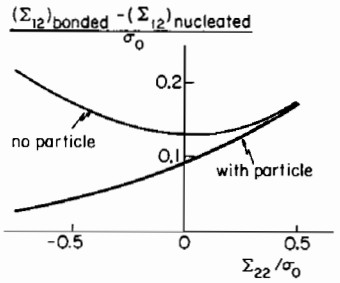

FIG. 14. Overall shear stress drop due to nucleation as a function of the superposed normal stress Σ_{22}, for $a/b = 0.25$.

voids, although there is slightly more softening behavior. A plot of the overall shear stress drop immediately following nucleation is shown in Fig. 14. This figure illustrates the strong influence of contact between particle and void surface in solids subject to shearing. Clearly, a significant superposed hydrostatic tension ($\Sigma_{22} > 0.5\sigma_0$ in the present model problem) is required before the effect of contact with the particle can be neglected. The results of Fig. 14 suggest that the component Σ_{22} should have a significant influence on the softening contribution due to nucleation in shear. This is borne out indirectly by the experiments conducted by COWIE *et al.* (1987).

4. ELLIPSOIDAL VOIDS UNDER SIMPLE SHEAR IN A LINEARLY VISCOUS MATERIAL

Several aspects of three-dimensional void growth in linearly viscous materials in simple shear are investigated in this section motivated by a desire to obtain a better understanding of the influence of voids under large amounts of shear as occurs, for example, in shear localization and beneath the surface of roller bearings. It is well known that an isolated traction-free ellipsoidal void subject to remote shearing remains ellipsoidal as it rotates and deforms and is amenable to an analysis based on ESHELBY's (1957) theory for ellipsoidal inhomogeneities. Such studies have been reported by MCCLINTOCK *et al.* (1966) for two-dimensional voids in plane strain flows and by BILBY and KOLBUSZEWSKI (1977) and FLECK and HUTCHINSON (1986) for initially spherical voids. In this section, the effect of particle contact on the deformation of the void is approximated in a way which preserves the feature that the voids evolve through a sequence of ellipsoidal shapes permitting continued use of Eshelby's solution. The focus in this section is on: (1) evolution to large shear strain, (2) the influence of initial void shape and orientation and (3) three-dimensional interpretation of two-dimensional results.

Calculations will be carried out for a material which is incompressible with the strain-rate relation

$$\dot{\varepsilon}_{ij} = \sigma'_{ij}/(2\mu), \tag{4.1}$$

where μ is the viscosity. The remote state is simple shear with superimposed hydrostatic stress Σ_m such that far from the void

$$\sigma_{11} = \sigma_{22} = \sigma_{33} = \Sigma_m, \quad \sigma_{12} = \Sigma_{12},$$
$$\dot{u}_1 = \dot{\gamma} x_2, \quad \dot{u}_2 = \dot{u}_3 = 0,$$
$$\dot{\varepsilon}_{12} = \tfrac{1}{2}\dot{\gamma}, \quad \dot{\omega}_{12} = \tfrac{1}{2}\dot{\gamma}. \tag{4.2}$$

The remote shear strain measure γ is defined by the above equation and is also interpreted in the insert in Fig. 15.

The void is imagined to be nucleated from a bonded, rigid ellipsoidal particle of unit volume at $\gamma = 0$. The stress drop due to the presence of the void will be calculated as a function of γ, the drop being measured from the bonded particle whose orientation has evolved to that associated with the same value of γ. The overall stress history of the material with voids can therefore be directly compared with that for the material with bonded particles, assuming dilute concentrations of particles and voids nucleated from the particles.

To start, a general result is derived for the stress drop *relative to the uniform matrix* for an ellipsoidal inclusion of unit volume embedded in a uniform matrix which is subject to a prescribed remote strain rate $\dot{\mathbf{E}}$. HILL's (1965) notation and formalism for the class of Eshelby inclusion problems will be used. At this stage in the analysis the matrix is taken to be compressible and linearly viscous with

$$\dot{\boldsymbol{\varepsilon}} = M\boldsymbol{\sigma} \quad \text{and} \quad \boldsymbol{\sigma} = \mathbf{L}\dot{\boldsymbol{\varepsilon}}, \tag{4.3}$$

where standard vector-matrix notation is used for symmetric second-order tensors and diagonally symmetric fourth-order tensors. The uniform viscous properties of the bonded ellipsoidal inclusion are characterized by M^c and L^c, and the uniform stress and strain-rate inside the inclusion are denoted by $\boldsymbol{\sigma}^c$ and $\dot{\boldsymbol{\varepsilon}}^c$.

Following the procedure given in Section 2 and referring to the notation for the finite region in Fig. 2, let uniform straining $\dot{u}_i = \dot{E}_{ij}x_j$ be prescribed on A_R and define the stress drop relative to the block of uniform matrix within A_R as

$$\Delta\Sigma_{ij} = \int_{A_R} (\Sigma_{ik} - \sigma_{ik}) n_k x_j \, dA = \int_V (\Sigma_{ij} - \sigma_{ij}) \, dV, \tag{4.4}$$

where $\boldsymbol{\Sigma} = L\dot{\mathbf{E}}$ and the inclusion is taken to have unit volume. Next, form $\Delta\Sigma_{ij}\dot{E}_{ij}$ noting $\dot{u}_i = \dot{E}_{ij}x_j$ on A_R. Then, by the principle of virtual work

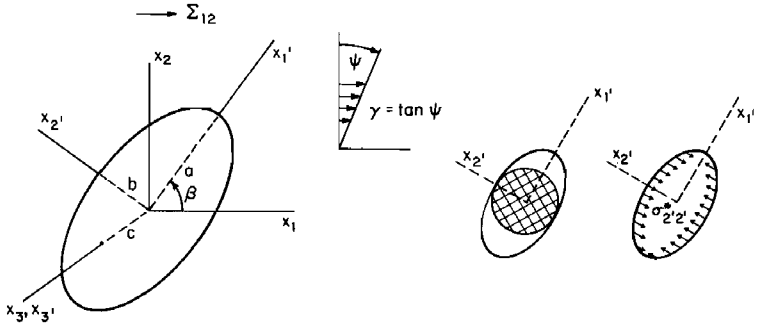

FIG. 15. Geometry for ellipsoidal voids in simple shear.

$$\Delta\Sigma_{ij}\dot{E}_{ij} = \int_V (\Sigma_{ij} - \sigma_{ij})\dot{\varepsilon}_{ij}\,\mathrm{d}V$$

$$= \int_{V_0} (\Sigma_{ij} - \sigma_{ij}^c)\dot{\varepsilon}_{ij}^c\,\mathrm{d}V + \int_{V_R} (\Sigma_{ij} - \sigma_{ij})\dot{\varepsilon}_{ij}\,\mathrm{d}V. \tag{4.5}$$

Now, noting $(\Sigma_{ij} - \sigma_{ij})\dot{\varepsilon}_{ij} = \sigma_{ij}(\dot{E}_{ij} - \dot{\varepsilon}_{ij})$ in V_R by reciprocity, and then by repeated applications of the principle of virtual work (recalling $\dot{u}_i = \dot{E}_{ij}x_j$ on A_R), one obtains

$$\int_{V_R} (\Sigma_{ij} - \sigma_{ij})\dot{\varepsilon}_{ij}\,\mathrm{d}V = -\int_{A_0} \sigma_{ik}n_k(\dot{E}_{ij}x_j - \dot{u}_i)\,\mathrm{d}A$$

$$= -\int_{V_0} \sigma_{ij}(\dot{E}_{ij} - \dot{\varepsilon}_{ij})\,\mathrm{d}A. \tag{4.6}$$

Lastly, letting $R \to \infty$ so that $\boldsymbol{\sigma}^c$ and $\dot{\boldsymbol{\varepsilon}}^c$ are uniform and taking V_0 as a unit volume, one obtains from (4.5) and (4.6)

$$\Delta\Sigma_{ij}\dot{E}_{ij} = \Sigma_{ij}\dot{\varepsilon}_{ij}^c - \sigma_{ij}^c\dot{E}_{ij}$$

$$= (L_{ijkl}\dot{\varepsilon}_{kl}^c - \sigma_{ij}^c)\dot{E}_{ij}. \tag{4.7}$$

It follows then by the linearity of the problem that

$$\Delta\boldsymbol{\Sigma} = L\dot{\boldsymbol{\varepsilon}}^c - \boldsymbol{\sigma}^c. \tag{4.8}$$

The similar result for an ellipsoidal void subject to uniform tractions $\sigma_{ij}^* n_j$ over its surface ($\mathbf{n}$ pointing into the void) is

$$\Delta\boldsymbol{\Sigma} = L\dot{\boldsymbol{\varepsilon}}^c - \boldsymbol{\sigma}^*. \tag{4.9}$$

A parallel derivation assuming prescribed uniform tractions, $\sigma_{ij}n_j = \Sigma_{ij}n_j$, on A_R leads to the result for the extra strain-rate due to the inclusion of unit volume relative to the uniform block as

$$\Delta\dot{\mathbf{E}} = M\Delta\boldsymbol{\Sigma} = \dot{\boldsymbol{\varepsilon}}^c - M\boldsymbol{\sigma}^c. \tag{4.10}$$

These results, which are implicit in the works of Eshelby and Hill, are now specialized to cases of interest here. It is convenient to use the special diagonally symmetric fourth-order tensors, M^* and $L^* = M^{*-1}$, introduced by HILL (1965) which relate the uniform strain rate $\dot{\boldsymbol{\varepsilon}}^*$ experienced by an ellipsoidal void resulting from uniform tractions $\sigma_{ij}^* n_j$ acting over its surface ($\mathbf{n}$ pointing into the void with no stress at infinity), i.e.

$$\dot{\boldsymbol{\varepsilon}}^* = -M^*\boldsymbol{\sigma}^* \quad \text{and} \quad \boldsymbol{\sigma}^* = -L^*\dot{\boldsymbol{\varepsilon}}^*. \tag{4.11}$$

For a bonded, rigid ellipsoidal particle, $\dot{\boldsymbol{\varepsilon}}^c = 0$ and (4.8) reduces to

$$\Delta\boldsymbol{\Sigma} = -\sigma^c = -(I + ML^*)\boldsymbol{\Sigma}, \tag{4.12}$$

where I is the identity matrix and the expression for $\boldsymbol{\sigma}^c$ is obtained readily from results in HILL's (1965) paper. When the particle is spherical and the matrix is isotropic and incompressible the deviator stress drop obtained from (4.12) is

$$\Delta\Sigma' = -\tfrac{5}{2}\Sigma', \tag{4.13}$$

which is opposite-signed from the stress deviator since the rigid particle raises the average stress.

For an ellipsoid void subject to uniform traction $\sigma^*_{ij}n_j$ on its surface with $\dot{\mathbf{E}}$ in the matrix at infinity (HILL, 1965)

$$\dot{\varepsilon}^c = (I+M^*L)\dot{\mathbf{E}} - M^*\boldsymbol{\sigma}^* \tag{4.14}$$

and (4.9) becomes

$$\Delta\boldsymbol{\Sigma} = (I+LM^*)(\boldsymbol{\Sigma}-\boldsymbol{\sigma}^*). \tag{4.15}$$

For a traction-free, spherical void in an incompressible isotropic matrix the deviator part of (4.15) reduces to

$$\Delta\boldsymbol{\Sigma}' = \tfrac{5}{3}\boldsymbol{\Sigma}'. \tag{4.16}$$

The total deviatoric stress drop of an unconstrained spherical void relative to a bonded spherical particle, both of unit volume, obtained as the difference between (4.16) and (4.13) is

$$\Delta\boldsymbol{\Sigma}' = \tfrac{25}{6}\boldsymbol{\Sigma}'. \tag{4.17}$$

When the evolution of the traction-free void indicates that one or more of the principal axes of the void diminish below the corresponding axes of the nucleating particle, contact between the void surface and particle will occur. This contact is modeled in the following approximate way. At any instant the constraint is modeled by application of a uniform traction $\sigma^*_{ij}n_j$ in the direction (or directions) of the principal axis (or axes) over the full surface of the void and by choosing this traction component (or components) to enforce the condition that the length of the corresponding axis (or axes) not diminish below that of the corresponding particle axis (or axes). For example, if the principal axis b of the unconstrained void in the $x_{2'}$ direction (see Fig. 15) is diminished below the corresponding axis of the particle, then a uniform traction derived from $\sigma^*_{2'2'}$ is applied to the void surface with $\sigma^*_{2'2'}$ chosen so that $\dot{b} = 0$. Enforcement of the particle constraint in this approximate manner permits the Eshelby solution to be applied exactly to the model since the void continues to evolve through a sequence of ellipsoidal shapes.

Application of the above procedure to a void which is instantaneously spherical with unit volume interacting with a rigid spherical particle of unit volume and which is subject to the remote field (4.2) gives the following. For $\Sigma_m > (10/3)\Sigma_{12}$ the void pulls away from the particle in all directions and the shear stress drop relative to the bonded particle is given by (4.17), i.e. $\Delta\Sigma_{12} = (25/6)\Sigma_{12}$. For

$$(5/18)\Sigma_{12} < \Sigma_m < (10/3)\Sigma_{12}, \tag{4.18}$$

contact occurs with only the constraint associated with $\sigma^*_{2'2'}$ active and the shear stress drop is found to be

$$\Delta\Sigma_{12} = \tfrac{25}{6}\Sigma_{12} - \tfrac{5}{22}[10\Sigma_{12} - 3\Sigma_m]. \tag{4.19}$$

For

$$-(5/2)\Sigma_{12} < \Sigma_m < (5/18)\Sigma_{12}, \tag{4.20}$$

contact occurs in the 2′ and 3′ directions and the shear stress drop is

$$\Delta\Sigma_{12} = \tfrac{25}{6}\Sigma_{12} - \tfrac{1}{24}[55\Sigma_{12} - 18\Sigma_m]. \tag{4.21}$$

While for $\Sigma_m < -(5/2)\Sigma_{12}$ the void surface and particle maintain contact everywhere and $\Delta\Sigma_{12} = 0$.

The procedures outlined above can be applied to calculate the evolution of the void and the associated stress drop, with or without void–particle contact. Numerical work is necessary when the configuration is not spherical; in particular, M^* must be computed using the basic Eshelby solution for each ellipsoidal shape and orientation and the evolution of the principal axes of the void and their orientation must be tracked. Details for the unconstrained void can be found in FLECK and HUTCHINSON (1986). Those for the constrained void, and for the bonded rigid particle which serves as a reference, are similar in most respects and will not be given here.

The evolution of an initially spherical void in the remote simple shearing stress field (4.2) is shown in Fig. 16. The orientation of the major axis of the void (refer to Fig. 15 for notation) and the shear stress drop are shown for three levels of Σ_m/Σ_{12}, while the lengths of the principal axes are only shown for $\Sigma_m = 0$. In each figure in this section, the shear stress drop $\Delta\Sigma_{12}$ is based on a void and particle with *initial* unit volume at $\gamma = 0$. It is not renormalized to a current unit volume at each γ. The stress drop is the total stress drop measured from the bonded rigid particle which coincides with the predictions (4.17) through (4.21) when $\gamma = 0$. The behavior of the unconstrained void is shown as dashed-line curves and the evolution of the shape and orientation were reported earlier by FLECK and HUTCHINSON (1986). With $\Sigma_m = 0$, the unconstrained void closes to an elliptical crack ($b \to 0$) when $\gamma = 1.76$. (In this

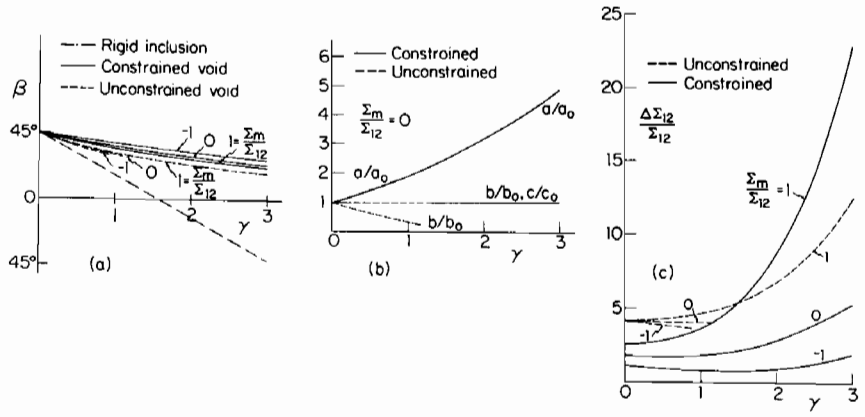

FIG. 16. Evolution with γ for a void nucleated as a sphere at $\gamma = 0$. (a) Orientation of major axis. (b) Major and minor axes. (c) Shear stress drop for void with unit volume at $\gamma = 0$.

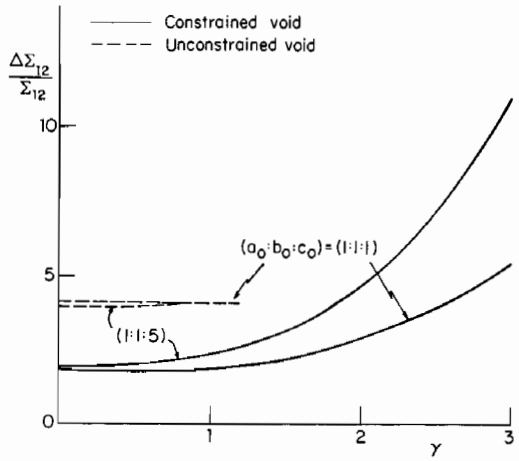

FIG. 17. Comparison of the shear stress drop for an initially spherical void with that for a nearly 2-D void ($a_0 : b_0 : c_0 = 1 : 1 : 5$). In each case the initial volume at $\gamma = 0$ is unity and $\Sigma_m = 0$.

section the calculations were terminated when b/b_0 dropped below 1/10.) The associated stress drop $\Delta\Sigma_{12}$ (which is normalized to unit *initial* volume) is virtually unchanged as γ increases even as the void becomes crack-like.

The main effect of the particle constraint is to prop open the void in the 2′ direction maintaining the initial length of that axis, b_0. The initial shear stress drop is less than that associated with the unconstrained void, but with increasing remote strain the shear stress drop slowly increases and for $\Sigma_m/\Sigma_{12} = 1$ eventually becomes larger than that for the unconstrained void. Thus, the model does give some evidence for a softening mechanism due to void deformation in shear of the type envisioned by TEIRLINCK *et al.* (1987).† However, the effect appears to be relatively small and only evident after fairly large shearing. For shear strains less than about unity there is virtually no effect when $\Sigma_m = 0$, consistent with the findings from the two-dimensional elastic–plastic calculations reported in the previous section.

The model can be used to obtain some sense of the relationship between quantities of interest calculated using a two-dimensional plane strain model with a cylindrical void and those calculated for a three-dimensional void. Figure 17 displays the evolution of the shear stress drop (based again on unit volume at $\gamma = 0$) under plane strain shearing ($\Sigma_m = 0$) for constrained and unconstrained voids which start out as spheres or as highly prolate ellipsoids with the long axis in the 3-direction ($a_0 : b_0 : c_0 = 1 : 1 : 5$). Presumably, the behavior of the highly prolate ellipsoids is close to the two-dimensional plane strain limit. The shear stress drop is clearly relatively independent of c/a, at least for shear strains less than about unity.

The behavior of a prolate ellipsoidal void ($a_0 : b_0 : c_0 = 3 : 1 : 1$) orientated with its long axis in the (x_1, x_2) plane is shown in Fig. 18. These results are for $\Sigma_m = 0$ and are determined for three starting orientations: $\beta = 0°$, 45° and 90°. Included in the figure is the behavior of the bonded rigid prolate particle which is used as the reference

†Since the stress drop is defined for a void of unit initial volume, the increase in stress drop with γ can be interpreted as an overall softening contribution.

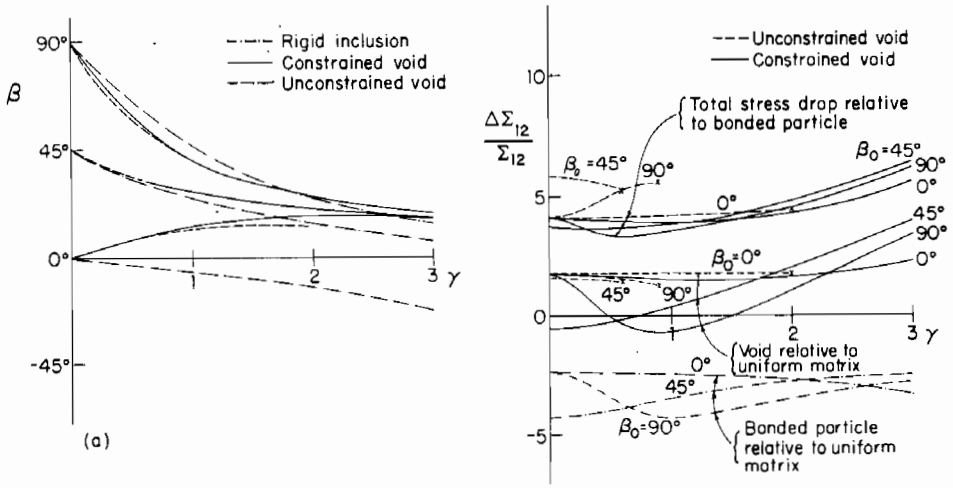

FIG. 18. Effect of initial orientation on subsequent evolution of orientation and stress drop of an initially prolate void ($a_0 : b_0 : c_0 = 3 : 1 : 1$) of unit volume at $\gamma = 0$.

in calculating the total shear stress drop. The shear stress drop of the bonded particle and that of the void relative to the uniform matrix are each shown to reveal the nature of the separate contributions to the total stress drop. The bonded rigid particle provides maximum reinforcement (i.e. most negative stress drop) when its long axis is aligned with the principal directions of straining, $\beta = \pm 45°$. The unconstrained voids close as γ increases and the curves are terminated when $b/b_0 = 1/10$. The stress drop of the unconstrained void relative to the uniform matrix is quite insensitive to the orientation of the void. The variation of the total stress drop $\Delta\Sigma_{12}$ mainly arises from the contribution due to the bonded particle. The constrained void displays almost no variation in total stress drop with initial orientation, but the drop is about twice that for the constrained void which starts as a sphere in Fig. 16.

5. CONCLUDING REMARKS

At zero mean stress, whether in shear or under axisymmetric straining, accounting for contact between the void surface and its nucleating particle results in a predicted reduction in softening of roughly a factor of two compared to a calculation which ignores such contact. Under distinctly negative mean stress states the effect is even larger. The subsequent growth of the void is also appreciably affected by contact between the void surface and the particle.

For the most part, phenomenological models of dilatational plasticity such as that of GURSON (1977) have been developed and calibrated using results for voids undergoing axisymmetric straining with no allowance for contact between void surface and particle. The present results for the stress drop under axisymmetric stress states agrees well with the stress drop determined from the Gurson model when the stress triaxiality exceeds about $X = 1/3$. (See HUTCHINSON and TVERGAARD, 1987, for a more

complete discussion when void–particle contact is ignored. The issue of isotropic hardening vs kinematic hardening brought out in Fig. 6 is unresolved.) At lower stress triaxiality and in shear the present results indicate that the Gurson model should overestimate the softening due to nucleation by as much as a factor of two.

Acknowledgements

The work of NAF and JWH was supported in part by the Materials Research Laboratory under Grant NSF-DMR-86-14003, by the National Science Foundation under Grant NSF-MSM-84-16392, and by the Division of Applied Sciences, Harvard University. The work of VT was supported by the Danish Technical Research Council through Grant 16-4006.M.

References

Bilby, B. A. and Kolbuszewski, M. L.	1977	*Proc. R. Soc.* (*Lond.*) **A355,** 335.
Brownrigg, A., Spitzig, W. A., Richmond, O., Teirlinck, D. and Embury, J. D.	1983	*Acta Metall.* **31,** 1141.
Budiansky, B., Hutchinson, J. W. and Slutsky, S.	1982	*Mechanics of Solids*, p. 13 (edited by H. G. Hopkins and M. J. Sewell), Pergamon Press, Oxford.
Cowie, J. G., Azrin, M. A. and Olson, G. B.	1987	Micro-void Formation During Shear Deformation of Ultrahigh Strength Steels, to be published in *Proc. of 34th Sagamore Army Research Conference.*
Duva, J. M.	1984	*J. Engng Mater. Technol.* **106,** 317.
Eshelby, J. D.	1957	*Proc. R. Soc.* (*Lond.*) **A241,** 376.
Fleck, N. A. and Hutchinson, J. W.	1986	*Proc. R. Soc.* (*Lond.*) **A407,** 435.
Gurson, A. L.	1977	*J. Engng Mater. Tech.* **99,** 2.
Hill, R.	1965	*J. Mech. Phys. Solids* **13,** 89.
Hutchinson, J. W.	1973	Numerical Solution of Nonlinear Structural Problems, AMD Vol 6, *American Soc. Mechanical Engineers*, 17.
Hutchinson, J. W. and Tvergaard, V.	1987	Softening Due to Void Nucleation in Metals, Report MECH-99, Division of Applied Sciences, Harvard University, to be published in ASTM STP.
McClintock, F. A., Kaplan, S. M. and Berg, C. A.	1966	*Int. J. Fracture Mech.* **2,** 614.
Needleman, A.	1987	*J. appl. Mech.* **54,** 525.
Needleman, A. and Rice, J. R.	1978	*Mechanics of Sheet Metal Forming* (edited by D. P. Koistinen and N.-M. Wang), Plenum Pub. Co., **237.**
Rice, J. R. and Tracey, D. M.	1969	*J. Mech. Phys. Solids* **17,** 201.
Teirlinck, D., Zok, P., Embury, J. D. and Ashby, M. F.	1987	Fracture-Mechanism Maps in Stress Space, to be published.
Tvergaard, V.	1976	*J. Mech. Phys. Solids* **24,** 291.

APPENDIX

ANALYSIS OF ISOLATED VOID UNDER REMOTE AXISYMMETRIC STRESSING

The various boundary value problems for the spherical particle and the nucleation of a spherical void in an unbounded, incompressible elastic–perfectly plastic matrix were posed in Section 2 along with identification of the quantities to be calculated. In what follows, the computational procedure is outlined for determining the stress and velocity distribution in the matrix. All other quantities of interest derive from these distributions.

Given remote yielding with stresses (2.2) and remote straining, $\dot{\mathbf{E}}$, the actual velocity field minimizes

$$\Phi(\dot{\mathbf{u}}) = \frac{1}{2}\int_V \dot{s}_{ij}\dot{\varepsilon}_{ij}\,\mathrm{d}V - \int_{A_0} \dot{T}_i\dot{u}_i\,\mathrm{d}A, \tag{A1}$$

where $\dot{\mathbf{T}}$ is prescribed on A_0 and the strain rates derived from $\dot{\mathbf{u}}$ approach $\dot{\mathbf{E}}$ as $r \to \infty$. This functional can be applied to the infinite region as it stands since $\dot{s}_{ij}\dot{\varepsilon}_{ij} = \mathrm{O}(r^{-6})$ for large r for the incompressible, elastic–perfectly plastic solid. The velocities are generated from a velocity potential according to

$$\dot{u}_r = -r^{-2}(\sin\theta)^{-1}(\Psi\sin\theta)_{,\theta}, \quad \dot{u}_\theta = r^{-1}\Psi_{,r}. \tag{A2}$$

The potential used in the calculations was

$$\Psi = -\tfrac{1}{4}\dot{E}_3 r^3 \sin 2\theta + a_0\cot\theta + \sum_{k=2,4,\ldots}\ \sum_{j=1,2,3,\ldots} a_{kj} r^{-j+1}[P_k(\cos\theta)]_{,\theta}, \tag{A3}$$

where the amplitude factors, a_0 and a_{ij}, were chosen to minimize Φ. The lead term in (A3) generates the remote uniform strain rate field while the second term with amplitude a_0 is the spherically symmetric contribution which has strain rates which vary like r^{-3}. The reduction of the minimization problem to a standard algebraic problem for the unknown amplitude factors follows the procedures spelled out previously in BUDIANSKY *et al.* (1982) and HUTCHINSON and TVERGAARD (1987). The numerical results reported in Section 2 were computed using 7 free amplitude factors (a_0, a_{21}, a_{22}, a_{23}, a_{41}, a_{42}, and a_{43}) to minimize Φ.

Several of the boundary value problems were subject to constraints on the velocities on A_0. For the case of the fully bonded rigid particle, the conditions $\dot{u}_r = \dot{u}_\theta = 0$ on A_0 were imposed on the velocities, which resulted in 5 linear constraints on the 7 amplitude factors. The limit stress distribution $\boldsymbol{\sigma}^0$ surrounding the rigid bonded particle was obtained by incrementing the remote strain using the uniform stress state $\boldsymbol{\Sigma}$ as an arbitrary starting point. After 10–15 increments on E_3, totaling several times ε_0, the stress distribution no longer changes and is identified with $\boldsymbol{\sigma}^0$. The stress rise due to the bonded particle in (2.11) is calculated using (2.10). During or subsequent to nucleation, contact between the void surface and the particle is modeled by enforcing $\dot{u}_r = 0$ at the equator of the void whenever the equatorial radius of the void decreased below that of the particle. This condition places one linear constraint on the amplitude factors.

FINITE ELEMENT ANALYSIS OF PERIODIC ARRAY OF VOIDS IN SHEAR

In the numerical analysis for the periodic array of particles undergoing simple shear (Fig. 8) finite strains are accounted for. The analysis is based on a Lagrangian formulation of the field equations, with the Cartesian x^i coordinate system used as reference. The Lagrangian strains are given by

$$\eta_{ij} = \tfrac{1}{2}(u_{ij} + u_{j,i} + u^k_{,i}u_{k,j}), \tag{A4}$$

where u^i are the displacement components on the reference base vectors and $(\ )_{,i}$ denotes covariant differentiation in the reference configuration. The contravariant components of the

Kirchhoff stress tensor τ^{ij} and the Cauchy stress tensor σ^{ij} are related by

$$\tau^{ij} = \sqrt{G/g}\sigma^{ij}, \tag{A5}$$

where g and G are the determinants for the metric tensors g_{ij} and G_{ij} in the reference configuration and the current configuration, respectively.

The finite strain generalization for elastic–perfectly plastic theory used here is analogous to that of HUTCHINSON (1973) for hardening materials. The incremental stress–strain relationship is of the form $\dot{\tau}^{ij} = L^{ijkl}\dot{\eta}_{kl}$, with the tensor of instantaneous moduli given by

$$L^{ijkl} = \frac{E}{1+\nu}\left\{\tfrac{1}{2}(G^{ik}G^{jl}+G^{il}G^{jk}) + \frac{\nu}{1-2\nu}G^{ij}G^{kl} - \beta\frac{3}{2}\frac{s^{ij}s^{kl}}{\sigma_0^2}\right\}$$
$$- \tfrac{1}{2}(G^{ik}\tau^{il}+G^{il}\tau^{jk}+G^{jl}\tau^{ik}+G^{jk}\tau^{il}), \tag{A6}$$

$$\beta = \begin{cases} 1, & \text{for} \quad \sigma_e = \sigma_0 \quad \text{and} \quad \dot{\sigma}_e = 0 \\ 0, & \text{for} \quad \sigma_e < \sigma_0 \quad \text{and} \quad \dot{\sigma}_e < 0. \end{cases} \tag{A7}$$

Here, $\sigma_e = (3s_{ij}s^{ij}/2)^{1/2}$ is the effective Mises stress and $s^{ij} = \tau^{ij} - G^{ij}\tau^k_k/3$.

A linear incremental solution procedure is employed in which the equations governing the stress increments $\Delta\tau^{ij}$, the strain increments $\Delta\eta_{ij}$, etc., are obtained by expanding the principle of virtual work about the current state, using (A4). To lowest order the incremental equation is

$$\int_V \{\Delta\tau^{ij}\delta\eta_{ij} + \tau^{ij}\Delta u^k_{,i}\delta u_{kj}\}\,\mathrm{d}V = \int_S \Delta T^i \delta u_i\,\mathrm{d}S - \left[\int_V \tau^{ij}\delta\eta_{ij}\,\mathrm{d}V - \int_S T^i\delta u_i\,\mathrm{d}S\right], \tag{A8}$$

where V and S are the volume and surface, respectively, of the body in the reference configuration, and T^i are contravariant components of the nominal surface tractions. The bracketed terms are included to prevent drifting of the solution away from the true equilibrium path. Furthermore, drifting of the stress state to a point slightly outside the yield surface is prevented by a proportional reduction of such stresses to a point on the yield surface.

Due to the periodicity described in connection with Fig. 8 it is only necessary to analyse the half-cell ABCD indicated in Fig. 8a. The boundary conditions on top of the region are specified by

$$\dot{u}^1 = \dot{U}_I, \quad \dot{u}^2 = \dot{U}_{II}, \quad \text{on} \quad \text{DC} \tag{A9}$$

where $\dot{U}_I$ and $\dot{U}_{II}$ are constants, $\dot{U}_I$ is prescribed, and $\dot{U}_{II}$ is calculated such that the average stress Σ_{22} has the prescribed value,

$$\Sigma_{22} \equiv \frac{1}{2b}\int_{-b}^{b} T^2\,\mathrm{d}x_1, \quad \Sigma_{12} = \frac{1}{2b}\int_{-b}^{b} T^1\,\mathrm{d}x_1, \quad \text{on} \quad \text{DC}. \tag{A10}$$

The periodicity and symmetry conditions on AC, BD and AB are such that equilibrium and compatibility with the neighboring cells is satisfied. This is expressed by using the length measuring coordinates ξ_1, ξ_2, η_1 and η_2 (see Fig. 8a)

$$u^1(\xi_1) = u^1(\xi_2), \qquad u^2(\xi_1) = u^2(\xi_2), \tag{A11}$$

$$T^1(\xi_1) = -T^1(\xi_2), \quad T^2(\xi_1) = -T^2(\xi_2), \tag{A12}$$

$$u^1(\eta_1) = -u^1(\eta_2), \quad u^2(\eta_1) = -u^2(\eta_2), \tag{A13}$$

$$T^1(\eta_1) = T^1(\eta_2), \qquad T^2(\eta_1) = T^2(\eta_2). \tag{A14}$$

From (A11) and (A13) it follows that the displacements vanish at points A and B, and at the center of the particle.

At the void surface, $(x^1)^2 + (x^2)^2 = a^2$, the conditions depend on whether or not there is a

particle. If there is no particle, the conditions are

$$\dot{T}^1 = \dot{T}^2 = 0. \tag{A15}$$

In the case where there is a particle, the current angle between the x^1-axis and the radius through a surface point is denoted by ϕ. Then, for a bonded particle, the conditions are

$$\dot{u}^1 \cos\phi + \dot{u}^2 \sin\phi = 0, \quad -\dot{u}^1 \sin\phi + \dot{u}^2 \cos\phi = a\dot{\Psi}, \tag{A16}$$

where $\dot{\Psi}$ is the incremental angle of rotation of the particle, which is determined such that the resultant moment acting on the particle is zero.

At nucleation all points on the void surface are simultaneously released from the particle, and the surface tractions are stepped down to zero in a few subsequent increments. At points, where the radius decreases below a, sliding contact with the particle is assumed, described by

$$\dot{u}^1 \cos\phi + \dot{u}^2 \sin\phi = 0, \quad -\dot{T}^1 \sin\phi + \dot{T}^2 \cos\phi = 0. \tag{A17}$$

The point remains in contact as long as the normal stress is compressive. Other points of the void surface that are not in contact with the particle satisfy (A15).

An approximate solution of the equilibrium equation (A8) is obtained by the finite element method, using the boundary conditions (A9)–(A17). In the solutions a special Rayleigh–Ritz finite element method (TVERGAARD, 1976) is used to find the edge displacements according to the periodicity conditions (A11)–(A14), the displacement $\dot{U}_{II}$ in (A9), and the particle rotation $\dot{\Psi}$ in (A16).

The initial geometry of the region analysed is shown in Fig. 11 for a case where $a/b = 0.25$ and $c/b = 3$. The mesh used for the finite element solution is shown in the figure, where each quadrilateral consists of four constant strain triangular elements.